

We truly appreciate all comments and constructive revisions from all authors. Below is an explanation, point by point and organized by reviewer, detailing how each comment has been addressed. The manuscript has been substantially modified to address all comments from the reviewers. We particularly stressed: 1) restructuring and shortening of all sections to make it less technical; and 2) better defined objectives which are stressed in the discussion.

Also, we are including two versions of the new manuscript, one annotated and showing the changes to the previous version, and a clean one with all changes accepted. Additionally a total of 4 figures have been modified following some of the comments from the reviewers and are also attached here.

Reviewer #1:

- 1. In Figure 4 (a), could you explain why you use 200 MHz instead of 100 MHz for GPR analysis?

Most of the profiles shown in this paper were collected using the entire array of antennas available (i.e. 50, 100 and 200 MHz). The 50 MHz antennas however malfunctioned during the end of the campaign and therefore were unfortunately not available when investigating "deep peat" sites. For brevity purposes, only one frequency per profile is shown. Since Figure 4 corresponds to a very shallow site, we chose to display the frequency that provides best vertical resolution for shallow depths. The 200 MHz antenna has the lowest depth of penetration while providing the best vertical resolution (plus the smallest ground coupling effect) and for that reason is chosen here since we are targeting a minimum thickness of the peat column of only a few cm.

- 2. In Figure 5 (a), "TG2.1-TG.3" is misspelled and "3.4 m" is too large.

Misspelling in the legend is now corrected. We do not however understand the reference to 3.4 m being too large. This reading corresponds to the depth of the peat-clay interface as detected from coring.

- 3. In Figure 7, what does black diamond mean?

Black diamonds have now been removed from the figure.

Reviewer #2:

- 1. Organization This paper has much content about technical method and its results on "Discussion". I think it is not a proper article. Please consider reconstructing this section into two sections, Methods and Discussion. Moreover, the paper lacks information about how to estimate peat thickness by using the GPR and ERI data. I suggest the authors should add more information in the Introduction and clearly explain it in Methods.

We agree that the original version of the paper was perhaps too heavy on methodology. For that reason the introduction has been rewritten to focus on the importance of peatlands and current estimation of peat volume and thickness in peatlands. A lot of specific details on methodology have been removed to stress those points above. Also, see next comment for more specifics on how the introduction has now been focused on peat thickness characterization as suggested by the reviewer. The methods section has also been considerably shortened particularly some of the more technical details on inversion of ERI datasets.

The discussion section has been also substantially rewritten and new subsections have been added to stress results and implications and many of the more technical aspects have been removed, such as some particularities on how picks for both GPR and ERI datasets were conducted. See more details about these changes in point number 4 for Reviewer 3. Some remarks have been also added to the abstract and conclusions to clarify objectives and accomplishments.

- 2. Introduction The paper is currently too “heavy” in “Introduction”. The authors should just briefly describe the importance of peatland and put the focus more on the methodology part, for example, about the conventional methods used for peatland and its technical problems, and also the estimation of peat thickness using the GPR and the ERI.

See response to previous comment above. The introduction has been shorten and mostly rewritten to exactly stress peatland importance (paragraph 1); traditional approaches to peat thickness (and problems related to those approaches) (paragraph 2); previous studies using geophysical methods used in this study and justification for applicability in tropical systems and focusing on peat thickness characterization (paragraph 3), and objectives of the paper (paragraph 4). Following the reviewer suggestion, paragraph 3 is now rewritten and focused on previous studies using GPR and ERI to characterize peat thickness.

- 3. Objective The objective is not clear, because the estimation is not alluded on Introduction. I think that this paper will be more suitable for this journal if authors develop more accurate estimation by using the GPR and the ERI data in a woody peatland.

As described above the paragraphs preceding the last paragraph in the introduction are now focused on peat thickness characterization, including several recent studies using GPR to compare estimates from traditional coring methods. While we stress the results from those studies as related to accuracy when comparing methods at larger (basin) scales, we intend to focus on smaller scales and exemplify how our datasets could be extrapolated to larger scale investigations. The objectives have been also slightly modified to stress that the intention of the paper is to investigate the potential of the methods for peat thickness characterization.

- 4. Discussion In the results of peat thickness estimation (Fig. 9), the author describes the appropriateness of the estimation, but the values have a quite large variation. Readers will interpret the estimation as not accurate and cannot be used. In order to avoid this kind of misunderstanding, the author should explain about the error. Additionally, the results should be described in “Results” section.

As previously explained and following previous comments from the reviewer, the discussion has been substantially modified. In general we have added subsections to make things clearer. We have included in several instances how GPR is able to detect thickness at cm vertical resolution, while ERI is not as suitable for accurately detecting this boundary (i.e. paragraph 2 of the Discussion). The main advantage of ERI however is the fact that is less limited when investigating deep peat columns (i.e. where the GPR signal is not able to reach). In that regard our error analysis in the discussion section also reflects this showing average errors of +/- 0.05 m for GPR while exceeding 0.5 m for ERI. For that reason only our GPR estimates are used to quantify changes in C stock estimates as described in paragraph 5 of the Discussion.

- 5. Specific comments 1. Please add the explanation the calculation of carbon of Table 2.

If we understand this comment correctly, further details on Carbon analysis are included in the methods section (section 3.3).

- 6. L292 & L299: Generally, the citation does not list it in “Results”.

If we understand this comment correctly, citations should not be included in the results section. For that reason in both cases they have been removed and/or moved to the discussion section.

- 7. Figure 2: What is “woody layers?”?

In order to avoid confusion, the term "woody layer" in Figure 2 has now been replaced with "woody area" as explained in the text (section 4.1).

-8. Figure 2 and 5, 6: Water table elevation is water table depth

"Water table elevation" has been replaced with "water table depth" in all figures.

Reviewer #3:

- 1. The paper presents interesting data on a critical issue: estimation of carbon stocks of tropical peatlands. However, the paper, as currently written, is not well structured for Biogeoscience discussion. It is too technical and focused on the geophysical methods. The paper should be restructured and extended for a publication in Biogeoscience discussions or sent to another journal more focused on geophysical methods. The authors should, in the discussion section, present direct answers to the objectives stated at the end of the introduction. The demonstration of how geophysical methods help to increase the accuracy of peat C storage should be more clearly presented.

As further detailed in the responses to the comments from Reviewer 2 the introduction has been restructured and many of the more technical details related to the methodology part have been removed. The methods section has been substantially shortened, particularly the ERI section, where some of the more technical details on inversion of datasets have now been removed.

Furthermore, we have now included subsections in the discussion with a clear mention to the objectives as related to the text in the end of the introduction. We hope this helps clarifying how the discussion is answering those objectives. The specific subsections are: peat thickness, peat C stocks, peat formation, and peat matrix.

- 2. A great interest of this study and geophysical method is, as stated in the conclusion, the ability to detect wood buttress in the peat matrix. These features are critical in tropical peat system and strongly influences peat density and carbon stocks estimates. The author should emphasize this aspect and how it could actually improve the carbon stock estimates.

Although the feature described in the end of the discussion seems to be rather isolated in our dataset we have now expanded our interpretation of buttressed tress by including some recent study on tip-up pools by Dommain et al, 2005 (see reference list in manuscript). We have also included the importance of such features from a perspective of carbon accumulation rates and paleo-environmental reconstructions.

- 3. The results description is too detailed.

Certain details of the results section have been shorten, particularly as related to some technical aspects of GPR data processing (i.e. migration), or ERI results as compared to values

obtained in northern systems. Description of figures has not been modified since we believe that they are fairly concise and they mainly stress results as related to peat thickness and thus are critical for the points risen in the discussion.

- 4. The discussion section should be shorten and structured and emphasize a few clear points.

As already explained in our response to comment 1 from reviewer 2, the discussion section has been substantially rewritten and reorganized to make it shorter, less technical, and to emphasize objectives as stated in the end of the introduction. These objective are highlighted as the headers of subsections as follows: 1) peat thickness; 2) peat C stocks; 3) peat formation; and 4) peat matrix.

We have also deleted substantial parts of the discussion for brevity purposes (i.e. some of the discussion towards the end as related to the properties of the peat matrix, see annotated version).

- 5. Detailed comments: Table 1: Please provide the peat bulk density values that were measured to calculate 'peat profile C stock' (p202, l3).

Peat bulk density values are now included in Table 2

-6. P203, l19-21, How do the authors relate resistivity values to ionic concentration?

First we would like to clarify that we do not intend to generate a formal relationship between resistivity and ionic concentration. As mentioned in the paper however, and as explained in previous research in other peatlands ionic concentrations may dictate bulk resistivity values. For instance, resistivity values for the upper layer of the peat column are comparable

with values obtained in northern peatlands and partly attributed to the low ionic concentration of the peat pore water in these northern systems.

Reviewer 4:

- This paper has explained the prospects of the use of ground penetrating radar (GPR) and electrical resistivity imaging (ERI) as an alternative approach of peat depth and peat carbon estimates as well as for characterization of other features of tropical peatland. I gathered have a clear picture of what this technology can do for peat depth estimate and it's a good enough information. This paper will be more powerful if the estimate of C stock is more clearly explained – what these two techniques can and can not do in terms of C stock estimate.

As explained earlier the paper has been substantially reworded and reorganized to stress the potential of the methods as related to C stock estimation. Besides from all the changes explained above (particularly in the discussion section), the text in the discussion related to our first objective (refine peat thickness and C stocks) has been substantially reduced in size by removing some technicalities in the approach, and reworded to stress more clearly how each method can be used to refine peat thickness estimates and consequently C stock estimates. The discussion now also includes a direct mention to the objectives as sub-headers to stress how those are addressed in the paper. We particularly stress both the potential and limitations of the methods. Furthermore, changes to the abstract and conclusions have been also included to stress the potential and limitations of the methods and the relation between our peat thickness estimate and C stock determination.

- Specific Comments:

1. Title: I raised expectation that this technique can speed up the estimate of peat C stock, but I did not get satisfactory explanation on this aspect. Be more specific in the title.

We have now replaced "carbon stocks" with "peat thickness" in the title to be more specific about the objectives outlines in the manuscript.

2. Abstract, last sentence: Make a clearer statement whether with the absence of wood layers etc. this technology can provide a reliable estimate of peat C content and how close the estimate is compared to the analytical technique (peat sample analyses of bulk density and C content).

Following some of the previous comments we have now included a few sentences that specifically provide a quantification of our estimates in the abstract (see annotated manuscript version).

3. Introduction

Line 23: Indonesian peat area estimate is no longer 21 Mha (Wahyunto et al. 2003, 2004).

Ritung et al. 2011 (in which Wahyunto is a coauthor) has made a new estimate of 14.9 Mha.

This new estimate is used for national development agenda such as the moratorium map.

Please check at:

http://bbsdlp.litbang.pertanian.go.id/index.php?option=com_phocadownload&view=category&id=32:peta-lahan-gambut-indonesia&Itemid=185

We have now included that estimate and reference in the text.

Page 194, line 12: Include the more recent papers such as Ballhorn et al. (2012).

Following some of the previous comments, this sentence has now been removed and therefore the reference suggested is no longer applicable here.

Page 194, line 24-27, explain which source of uncertainty among area, depth and volume that can be tackled by the proposed techniques. Can these technique potentially be adapted to airborne observation for speeding and improving the quality of conventional peat distribution and depth mapping?

We have now included the following sentence to address the reviewer's comment:
"Refinement of estimates on depth and volume of peat soils in Indonesia is the focus of this paper."

Page 195, line 7, "These peats accumulated at rapid rates". Usually people refer to slow rate of formation under natural condition and rapid rate of decomposition under drained peat.

Following some of the previous comments, this sentence has now been removed from the text.

Page 196, line 25, be clear whether carbon content is the main objective. Otherwise remove the phrase between brackets. It raised lots of expectation.

We agree with the comment and sentence in brackets has now been removed.

Page 197, line 2: (related to the second objective, above) I would expect that this technology will improve the assessment of peat subsidence and below ground C stock

change.

We also agree with the comment and the sentence in has been added to the text.

Page 197, line 26: “4-5 m of peat”, do you mean “4-5 m deep peat”?

Remark has now been added.

4. Methods

Page 199, line 4: “being 50-70 depending on peat type”. Do you mean “being 50-70 times”?

50-70 refers to the value of relative dielectric permittivity, which is unit less. We have included a remark in the text that the number refers to the value of relative dielectric permittivity.

Page 200, line 2: “particle size distribution”?

Grain has been replaced by particle as suggested here. Please note that the paragraph has now been placed in the end of the first paragraph under the description of ERI method (section 3.2).

Page 201, line 11-13: Either unclear or it involves grammatical problem.

Following some of the previous comments, this sentence has now been removed from the text and no longer applies.

Page 202: No explanation about C content determination technique.

We have no incorporated more information about the methodology used for C content estimation.

5. Table 2: Add a column of bulk density

Mean peat bulk density has now been added in Table 2.

6. Conclusions Make a clearer statement of what these technique can do about C content estimation, or clarify in the Introduction that it's not part of the objective.

We have added a few sentences in the conclusions to clarify accomplishments as related to peat thickness determination. Furthermore, a few sentences have been added in the third paragraph of the discussion to clarify that GPR/ERI are unable to directly estimate C content in peat samples and therefore extraction through coring and subsequent laboratory analysis are required.

1 **Imaging tropical peatlands in Indonesia using ground penetrating radar (GPR) and**
2 **electrical resistivity imaging (ERI): implications for ~~carbon stock~~peat thickness estimates**
3 **and peat soil characterization.**

4
5 Xavier Comas ^{*1}, Neil Terry ², Lee Slater ², Matthew Warren ³, Randy Kolka ⁴, Agus Kristijono
6 ⁵, Nana Sudiana ⁵, Dadan Nurjaman ⁵, Taryono Darusman ⁶.

7
8 ¹ Department of Geosciences, Florida Atlantic University, Davie, FL 33314 USA

9 ² Department of Earth & Environmental Sciences, Rutgers-Newark, Newark, NJ 07102 USA

10 ³ USDA Forest Service, Northern Research Station, Durham NH 03824 USA

11 ⁴ USDA Forest Service, Northern Research Station, Grand Rapids MN 55744 USA

12 ⁵ Indonesian Agency for Assessment and Application of Technology (BPPT), Jakarta 10340

13 Indonesia

14 ⁶ United States Forest Service affiliate, Puter Foundation

15

16 **Abstract**

17 Current estimates of carbon (C) storage in peatland systems worldwide indicate tropical
18 peatlands comprise about 15% of the global peat carbon pool. Such estimates are uncertain due
19 to data gaps regarding organic peat soil thickness, volume and C content. ~~Indonesian peatlands~~
20 ~~are considered the largest pool of tropical peat carbon (C), accounting for an estimated 65% of~~
21 ~~all tropical peat while being the largest source of carbon dioxide emissions from degrading peat~~
22 ~~worldwide, posing a major concern regarding long term sources of greenhouse gases to the~~
23 ~~atmosphere. W~~We combined a set of indirect geophysical methods (ground penetrating radar,
24 GPR, and electrical resistivity imaging, ERI) with direct observations ~~from using~~ core samples

25 sampling (including and C analysis) to better understand peatland thickness in West Kalimantan
26 (Indonesia) and determine how geophysical imaging may enhance traditional coring methods for
27 estimating peat thickness and C storage in a tropical peatland system in W. Kalimantan,
28 Indonesias. Both GPR and ERI methods demonstrated capability to estimate peat thickness in
29 tropical peat soils at a spatial resolution not feasible with traditional coring methods. GPR is able
30 to capture peat thickness variability at centimeter scale vertical resolution,- although peat
31 thickness determination was difficult for peat columns exceeding 5 m in the areas studied. due to
32 signal attenuation associated with thick clay-rich transitional horizons at the peat-mineral soil
33 interface. ERI methods were more successful for imaging deeper peatlands with thick
34 organomineral layers between peat and underlying mineral soil. Results obtained using GPR
35 methods indicate less than 3% variation in peat thickness (when compared to coring methods)
36 over low peat-mineral soil interface gradients (i.e. below 0.02 deg) and show a substantial
37 impacts in C storage estimates (i.e. up to 37 MgC/ha even for transects showing a difference
38 between GPR and coring estimates of 0.07 m in average peat thickness). The geophysical data
39 also provide information on peat matrix attributes such as thickness of organomineral horizons
40 between peat and underlying substrate, the presence of buried wood, buttressed trees or tip-up
41 pools and soil type. The use of GPR and ERI methods to image peat profiles at high resolution
42 can be used to further constrain quantification of peat C pools and aid-inform responsible
43 peatland management in Indonesia and elsewhere in the tropics.-
44

45 **1. Introduction**

46 Globally, tropical peatlands are estimated to store 89 PgC, equivalent to about one-tenth
47 of the current atmospheric carbon pool (Page et al. 2011). Indonesia contains about 47%the
48 largest -of the World's area of the world's tropical peatlands, with an previous estimates in the

49 ~~range of~~ ranging from 14.9 Mha (Ritung et al. 2011) to 21Mha ((Wahyunto et al. 2003, 2004,
50 Page et al. 2011). Indonesian peat swamps have been globally significant carbon sinks over the
51 past 15,000 years (Dommain et al. 2014), ~~and currently contain 65% of total tropical peat carbon~~
52 ~~. As most literature related to carbon cycling in peat soils has focused on boreal and arctic~~
53 ~~regions, many uncertainties exist regarding the role of tropical peat soils as a significant~~
54 ~~component of the global carbon cycle and their dynamics under a changing climate. Peatlands~~
55 ~~are also well known for other ecological functions such as regulating water supply and~~
56 ~~biodiversity conservation. Once significant carbon sinks, however~~ vast areas of Indonesian
57 peatlands are becoming large, long-term sources of greenhouse gases (primarily ~~carbon dioxide,~~
58 CO₂) to the atmosphere due to deforestation, drainage and/or peat fires (Page et al. 2002, van der
59 Werf et al. 2009). ~~When peat is drained, available oxygen stimulates microbial activity and~~
60 ~~organic matter decomposition. In addition, drained peat is highly vulnerable to fire and large~~
61 ~~areas of degraded Indonesian peatlands burn each year producing large scale CO₂ emissions and~~
62 ~~air pollution. Increased heterotrophic respiration and peat burning emits significant amounts of~~
63 ~~CO₂ to the atmosphere, contributing to global warming and climate change.~~ In a recent overview
64 of carbon distribution based on a 2008 inventory, Indonesia was considered the largest source of
65 CO₂ emissions from degrading peat worldwide, with values exceeding other large producers
66 such as China and the United States by almost one order of magnitude (Joosten 2009).
67 ~~Furthermore, emissions of other greenhouse gases (such as nitrous oxide, N₂O and methane,~~
68 ~~CH₄) may also be enhanced in peat soils by the addition of fertilizers or rewetting of drained~~
69 ~~peatlands. For all these reasons, Therefore,~~ Indonesia's peatlands are considered "hot spots" for
70 greenhouse gas emissions, ~~ecosystem services and biodiversity~~, and are ~~therefore targeted as~~
71 priority areas for climate mitigation strategies including programs such as Reducing Emissions
72 from Deforestation and Forest Degradation (or REDD+). However, ~~the lack of information~~

73 ~~on~~ data deficiencies regarding area, depth and volume and carbon density of Indonesian
74 peatlands and its carbon contributes to large uncertainties in patterns of peat carbon pools and
75 fluxes in carbon pools and fluxes at local to national scales. Such lack of information may also
76 contributing contribute to management decisions which exacerbate greenhouse emissions from
77 peatland degradation. Refinement of estimates on depth and volume of peat soils in Indonesia is
78 the focus of this paper.

79 Current estimates of C storage in global peatlands range between 528-694 Pg C (Hooijer
80 et al. 2006, Yu et al. 2010). Tropical and subtropical systems are estimated to comprise about
81 15% of the global peat carbon pool, from which about with Indonesia estimated to contain about
82 65% of tropical peat carbon of this pool is in Indonesia Page et al. (Page et al. 2011). ~~h~~ However,
83 these estimates are uncertain tentative show the highest range of uncertainty in terms of C
84 storage, mainly due to the uncertainties in peat thickness, volume and C content density at large
85 spatial scales, and because few attempts have been made to estimate tropical peatland carbon (C)
86 stores at local to global scales. reported between 82 and 92 Pg C is stored in tropical peatlands
87 worldwide, comprising about 15% of the global peat carbon pool. According to the same study,
88 Indonesian peatlands store about 57 PgC. Yu et al. (2010) estimated that tropical systems cover a
89 total area of 368,500 km² and represent 44-55 Pg of C. These peats accumulated at rapid rates
90 between 8,000-4,000 years ago to present (Yu et al. 2010). Estimating peat carbon storage
91 requires accurate volume measurements calculated from peat area and thickness. Page et al.
92 (2011) calculated peat volume for Indonesia using a mean peat depth of 5.5 m, which was based
93 on very few geographically biased data considering the scale at which the mean depth estimate
94 was applied: 206,950 km² throughout Indonesian Borneo (Kalimantan), Sumatra and Papua.
95 Perhaps the most accurate peat volume measurements published at a local scale in Indonesia
96 were reported by Jaenicke et al. (2008) who modeled peat depth using a combination of 542

97 discrete field measurements from direct coring, surface elevation models, satellite imagery and
98 spatial interpolation across four peat domes in Central Kalimantan. Despite the large number of
99 direct measurements of peat thickness, the uncertainty in carbon storage estimates ranged from
100 13-25%, which the authors attributed to bedrock unconformities not considered in the models of
101 peat volume derived from relationships between surface elevation and peat thickness (Jaenicke et
102 al. 2008). Most current efforts to model peat depth are based on the assumption that peat deposits
103 occur in uniform biconvex formations, despite evidence from field measurements indicating
104 considerable buried topography under the peat in some areas such as riverbeds and levees. For
105 example, surveys have shown mineral substrate topography changing as much as ~~3m~~ 2 m within
106 single transects (of less than one km) across several peat domes in Borneo (Konsultant 1998,
107 Dommain et al. 2010).

108 Near surface geophysical methods, particularly ground penetrating radar (GPR),
109 have been ~~extensively~~ used extensively in boreal peatland systems to explore many aspects
110 related to ~~peatland-peat~~ development and stratigraphy (Comas and Slater 2009), including peat
111 thickness: For example, see Comas and Slater (2009) for a review on the use of GPR for
112 peatland characterization. Recent studies specifically geared towards the characterization of peat
113 thickness and peat basin volume using GPR include a variety of field sites and typically
114 reconcile discrepancies in peat volume estimates of about 20% in peat volumes when
115 compared to traditional direct methods such as coring (Rosa et al. 2009, Parsekian et al. 2012,
116 Parry et al. 2014), (Worfield et al. 1986, Warner et al. 1990); the presence of natural soil pipes
117 (Holden et al. 2002) and pipelines in peat (Jol and Smith 1995); hydrogeology and pool
118 formation in peatlands (Slater and Reeve 2002, Comas et al. 2005b, Kettridge et al. 2008, Comas
119 et al. 2011b); geoelectrical properties of the peat matrix (Theimer et al. 1994, Comas and Slater
120 2004); peatland evolution (Comas et al. 2004, Kettridge et al. 2012); and biogenic gas

Formatted: Indent: First line: 0.5"

121 ~~distribution and dynamics in peat (Comas et al. 2005a, 2007, 2008, Parsekian et al. 2010, Comas~~
122 ~~et al. 2011a, Parsekian et al. 2011). The pore waters of peat soils in ombrotrophic boreal~~
123 ~~peatlands (typically being $200 \mu\text{S cm}^{-1}$ or less) are characterized by low fluid electrical~~
124 ~~conductivity, resulting in GPR investigation depths of up to 11 m (Slater and Reeve 2002).~~
125 Electrical resistivity imaging (ERI) has also been used in boreal systems for investigating several
126 aspects of peatland stratigraphy and hydrogeology (Meyer 1989, Slater and Reeve 2002, Comas
127 et al. 2004, Comas et al. 2011), however no studies to our knowledge have focused on peat
128 thickness characterization using ERI and hydrogeology (Slater and Reeve 2002), peatland
129 evolution (Comas et al. 2011) and biogenic gas distribution and dynamics in peat soils (Slater et
130 al. 2007).

131 Electrical conductivity of peat typically increases with depth in boreal systems due to
132 increased dissolved ion concentration and the underlying mineral soil usually exhibits a strong
133 electrical contrast to the terrestrial peat (Slater and Reeve 2002). ~~While~~ Although all
134 these numerous previous studies have been conducted in used GPR and ERI methodologies
135 to study peatland attributes in boreal systems, the use of these techniques in tropical systems has
136 not been reported. Although differences in peat types, terrain and/or vegetation cover between
137 boreal and tropical systems must be considered, similarities in peat electromagnetic and
138 electrical properties are anticipated, supporting the use of GPR and ERI methods for mapping
139 tropical peatlands and underlying buried topography. Here we report the use of a combination of
140 GPR and ERI methods to obtain high resolution profiles of peat layers in West Kalimantan,
141 Indonesia. ~~peatlands and although differences in peat types, terrain and/or vegetation cover~~
142 between boreal and tropical systems must be considered, we anticipate overall physical
143 properties of peat (which control electromagnetic and electrical properties) to be similar in
144 tropical systems thus Such observations supporting the use of GPR and ERI methods for mapping

145 | ~~tropical peatlands, although differences in peat types, terrain and/or vegetation cover between~~
146 | ~~boreal and tropical systems must be considered.~~
147 | ~~——— To our knowledge, we report the first study using a combination of GPR and ERI to~~
148 | ~~better characterize peatland systems in the tropics.~~ The objectives of this study were to 1) test the
149 | potential of GPR and ERI for estimate-estimating peat thickness in a non-invasive and spatially
150 | continuous way at a resolution previously unreported for tropical peatlands; and 2) evaluate
151 | whether certain information on geological settings and/or peat composition (~~related to carbon~~
152 | ~~content~~) can be drawn from these methods. The ultimate aim of the approach presented here is to
153 | demonstrate the applicability of geophysical methods to investigate tropical peat systems, and to
154 | highlight potential for improved increase the accuracy of peat C storage estimates at scales larger
155 | than compared relative to those estimates derived from traditional coring methods. Advancing ~~in~~
156 | this knowledge could potentially aid responsible inform peatland management decisions in
157 | Indonesia. and improve the assessments of peat subsidence and C stock changes and below
158 | ground C stock exchange.

159

160 | **2. Field sites****Methods**

161 | **2.1 Field Sites**

162

163 | Two peatland sites located in the West Kalimantan Province were chosen for this study:
164 | Tanjung Gunung (Sejahtera village, Kayong Utara District); and Pelang (Pelang village,
165 | Ketapang District). Both sites had been previously ~~visited by~~ investigated by USFS (United
166 | States Forest Service) collaborators and were known to contain variable peat thickness and
167 | multiple landcover types, while providing relatively easy access. The Tanjung Gunung site
168 | (hereafter referred to as TG) is adjacent to Gunung Palung National Park and its natural

169 resources have been heavily exploited by the local community for decades. Within the TG site,
170 two areas along the same peat formation were studied: a thinned, degraded forest (TG1) and a
171 mature rubber plantation which is located at the edge of the peat formation (TG2). The
172 physiographic terrain at TG is a 6 km wide swamp peatland known as Mendawai, MDW
173 (RePPProT, Regional Physical Planning Programme for Transmigration, (1990) that is
174 characterized by shallow peat. Kahayan (KHY) peaty alluvial plains are also formed along the
175 seaward edges of MDW (inset in Figure 1). Although the two selected study sites (TG1 and
176 TG2) are only approximately 1 km apart and are both situated in a transition zone between KHY
177 and MDW ecosystems, differences exist in terms of thickness of peat and organomineral
178 transitional layers and water table depth. While TG1 is characterized by MDW properties (i.e.
179 shallow peat swamps), TG2 is characterized by a mixture of MDW and KHY properties,
180 including landforms such as coalescent estuarine and riverine plains with lithologies that include
181 alluvium and marine sediments.

182 At the Pelang forest site (hereafter referred to as P), two areas along the same peat
183 formation were also studied: a thinned, degraded forest occurring on approximately 4-5m ~~deep of~~
184 peat (P1), which transitioned to a cleared area covered in secondary ferns and grasses, and a
185 degraded forest (P2) heavily used by a local village occurring on very deep peat (>9m).
186 Compared to the Tanjung Gunung sites (TG1 and TG2), Pelang Forest sites are characterized by
187 extensive peatlands over about 20 km x 20 km (inset in Figure1), forming three types of peat
188 ecosystems: a) Klaru (KLR) or permanently water logged peaty floodplains; b) Gambut (GBT)
189 or deeper dome-shaped peat swamp; and c) Mendawai (MDW) or shallower peat swamp.
190 Similar to the previous sites at TG, Kahayan (KHY) peaty alluvial plains are also formed along
191 the seaward edges of MDW (Figure 1). Two measurement sites were also selected at this
192 location and included P1 (located at a boundary zone of GBT and MDW), whereas site P2 is

193 located within GBT. The results of 2D resistivity measurements described below show
194 significant differences in these two ecosystems. Additional specifications for each study site are
195 summarized in Table 1, including a description of the landcover, average peat depth, and land
196 system after RePPProT (1990).

197

198 **3. Methods**

199 **3.1.2.2. Ground Penetrating Radar**

200 Ground penetrating radar (GPR) is a fast, reliable, and inexpensive geophysical method
201 for non-destructive mapping of shallow subsurface features in peatlands at scales ranging from
202 kilometers for geological features influencing peatland hydrology such as eskers (Comas et al.
203 2011), to centimeters for determination of bubble distribution in peat blocks at the laboratory
204 scale (Comas and Slater 2007). The GPR technique involves the transmission of short pulses of
205 high frequency electromagnetic (EM) energy into the ground, and measurement of the energy
206 reflected from interfaces between subsurface materials with contrasting electrical properties. In
207 the most common deployment, one antenna (the transmitter) radiates short pulses of EM waves,
208 and the other antenna (the receiver) measures the reflected signal as a function of time.

209 Reflections are primarily caused by changes in water content, which in turn are determined by
210 sediment type and soil density. Reliable estimates of EM wave velocity (v), primarily controlled
211 by relative dielectric permittivity $\epsilon_{r(b)}$, are required to convert the EM wave travel times recorded
212 by GPR to depths of significant reflectors. Due to the high water content of peat soils, $\epsilon_{r(b)}$ of

213 peat is very high compared to inorganic mineral soils, being reaching values of 50-70 depending
214 on peat type. When $\epsilon_{r(b)}$ is generally well constrained from velocity analysis, estimation of peat
215 depth is typically accurate to within ~20 cm (Parsekian et al. 2012).

216 ———GPR surveys were performed using a Mala-RAMAC system with 50, 100, and 200 ~~and~~
217 ~~50~~-MHz antennas, with the 100 MHz antennas proving the best compromise between depth of
218 investigation and resolution. Malfunctioning of the 50 MHz antennas towards the end of the
219 campaign prevented testing depth of penetration for this frequency at study sites with thicker
220 peat columns. The spacing between traces was 0.2 m and 16 stacks (or replicates) were used for
221 each trace. Two types of surface GPR surveys were performed: 1) common offset surveys, where
222 both transmitter and receiver antennas are kept at a constant distance as they are moved along
223 transects; and 2) common mid-point (CMP) measurements where transmitter and receiver are
224 separated incrementally to larger distances. ~~While~~ ~~e~~Common offset surveys ~~were~~ ~~are~~ ~~frequently~~
225 used for subsurface imaging purposes (since profiles resemble a geological cross-section where
226 depth is expressed as a travel time of the EM wave), whereas CMPs ~~were~~ ~~are~~ used for velocity
227 estimation.

228

229

230

231

3.2.2.3 **Electrical Resistivity Imaging**

232

233

234

235

236

237

238

239

ERI is a method for generating images of the variation in electrical resistivity in either 2
or 3 dimensions below a line or grid of electrodes placed at the earth's surface. Data are acquired
by measuring the voltage differences between electrode pairs in response to current injection
between additional electrode pairs. Numerical methods are used to solve the Poisson equation
relating the theoretical voltages at the electrodes to the distribution of resistivity in the
subsurface. Inverse methods are used to find a model for the subsurface resistivity structure that
is consistent with the recorded field data and also conforming to model constraints imposed
(typically the resistivity structure varies smoothly). The resulting resistivity structure describes

Formatted: Font: Bold

Formatted: Font: Bold

240 variations in the ability of subsurface soils and rocks to conduct an electrical current. The
241 resistivity is strongly controlled by water content, chemical composition of the pore water and
242 soil surface area/grain [particle](#) size distribution.

243 Electrical resistivity imaging was conducted using a four electrode Wenner configuration
244 with both 1 m and 2 m electrode spacing and providing maximum imaged depths of about 16 m.
245 The imaging depth was estimated from the model resolution matrix (Menke 1989) ~~(see Binley~~
246 ~~and Kemna (2005) for further details)~~ that depicted relatively good resolution within this region
247 when compared with the rest of the modeling domain. Measurements were performed using an
248 ARES (Automatic Resistivity System) G4 2A resistivity meter with a 48 multi-electrode switch
249 box. Inversion and forward simulations were performed with R2 [software](#) written by Andrew
250 Binley (Lancaster University). R2 uses an iterative finite element method to estimate resistivity
251 values at user-specified element locations in a finite element mesh. The regularization was based
252 on the popular smoothness constrained approach used to solve for the minimum structure
253 resistivity model that satisfies the data constraints.

254 A triangular mesh with ~~characteristic~~ length of one quarter of the ~~electrode~~ spacing at the
255 electrodes and growing larger toward the edges (to account for decaying model resolution) was
256 built using Gmsh, a three-dimensional finite element mesh [program](#) (Geuzaine and Remacle
257 2009). R2 requires an estimate of the error associated with each data point for convergence to be
258 evaluated. [For this purpose, it is best practice to collect reciprocal data \(a companion dataset](#)
259 [where current and potential electrodes are reversed\) to gain an informed estimate of the errors](#)
260 [associated with ERI measurements \(Slater et al., 2000\), since underestimating these errors can](#)
261 [produce image artifacts in the final ERI result which can mistakenly be interpreted as real](#)
262 [structures. In lieu of reciprocal data, we employed a 2% error model as input to R2 given the](#)
263 [low electrical noise expected in our remote field sites and stacking errors \(recorded on the](#)

264 ~~instrument) of less than 1.1%. The two sources of error in inversion of ERI data include forward~~
265 ~~modeling errors (resulting from discretization of the modeling domain) and observational error~~
266 ~~(error in the measured data themselves). For forward simulations, 3D current flow in a 2D earth~~
267 ~~(i.e. constant resistivity in the direction perpendicular to the model mesh) and singularity~~
268 ~~removal were applied (Lowry et al. 1989). Forward modeling errors were assessed through a~~
269 ~~forward simulation of the survey parameters in a 100 ohm-m earth. A mean error of 0.083%~~
270 ~~with standard deviation of 0.12% and a maximum of 1.1% were observed. Errors based on 2 data~~
271 ~~stacks averaged under 1% for all datasets, however this type of repeatability assessment typically~~
272 ~~underestimates the true observational error, and best practice is to collect reciprocal data for error~~
273 ~~estimation (Slater et al. 2000). Due to time limitations and the priority given to collecting other~~
274 ~~data during this campaign, no reciprocal data were collected. Therefore, for the purpose of the~~
275 ~~inversions, we chose an observational error model of 2% of the measured transfer resistance~~
276 ~~values given the low electrical noise expected in these remote environments, the small stacking~~
277 ~~errors, and experimentation with trial inversions that converged within 2 to 6 iterations using this~~
278 ~~error model.~~

279 ~~—— It is possible to specify regularization disconnects where no smoothing is to be applied in~~
280 ~~the model space (for example, where sharp lithological boundaries are expected). This approach~~
281 ~~has been demonstrated for engineered structures (Slater and Binley 2006). More recently, Coseia~~
282 ~~et al. (2011) removed smoothness constraints from resistivity images along a well-defined clay~~
283 ~~layer boundary. Application of regularization disconnects at the peat-mineral soil contact~~
284 ~~identified by GPR were considered and experimental inversions were performed. However these~~
285 ~~inversions either failed to converge or yielded unrealistic results. The most likely explanation~~
286 ~~for this observation is that the peat-mineral soil contact is actually smooth in terms of electrical~~
287 ~~conductivity, due to ionic transport upward into the peat from the underlying mineral soil (Slater~~

288 ~~and Reeve 2002). Although increasingly popular for constraining resistivity inverse models,~~
289 ~~enforcement of inappropriate regularization disconnects may in fact yield erroneous results when~~
290 ~~used inappropriately (Robinson et al. 2013). Thus, no regularization disconnects were used in~~
291 ~~model constraints.~~

292

293 ~~32.34.~~ **Coring**

294 A total of nine core samples were obtained along the linear transects established for
295 geophysical surveys using an Eijkelkamp Russian style peat auger inserted vertically into the
296 peat layer. Representative 5 cm peat soil subsamples were taken at depth intervals 0-30, 30-50,
297 50-100 cm and each subsequent 100 cm interval until mineral substrate was reached. After
298 extraction of core samples, water tables were directly measured using a measuring tape. The
299 length of the sampling device was 9 m ~~total~~ so detection of any deeper boundaries below 9 m
300 using direct methods was not possible. Peat layers were described in the field as “peat”,
301 “transitional” (a mixing horizon of peat and mineral soil) and “mineral soil” (mostly marine
302 derived fine silt and clay), which represented underlying mineral substrate. The 5 cm
303 subsamples were oven dried at 60 °C until constant weight was achieved, and weighed for bulk
304 density determination. Peat samples were then-and- sent to the USFS Northern Research Station
305 soil analysis laboratory for carbon analysis. S-am ples were finely ground, homogenized, and
306 analyzed for total C using a LECO TruSpec elemental CN analyzer (LECO Corp. St. Joseph
307 Michigan). Laboratory standards and analytical duplicates were run every 10 samples to ensure
308 data quality. ~~After extraction of core samples, water tables were directly measured using a~~
309 ~~measuring tape.~~ Peat carbon storage was calculated as:

310 $C_{\text{peat}} = V * C_d$

311 where C_{peat} is carbon storage (MgC ha^{-1}); V is peat volume (m^3), the product of area (ha) and
312 depth (cm); and C_d is peat carbon density (kg C m^{-3}), the product of peat bulk density (kg m^{-3})
313 and carbon content (%C).

315 **2.5 Geophysical surveys**

316 A set of geophysical surveys combined with direct sampling at each study site consisted of: 1)
317 one or more GPR common offset transects between 30-100 m long to identify the peat-mineral
318 soil reflector and other stratigraphic features (such as presence of wood layers or buried
319 buttressed trees) within the peat soil reflection record; 2) one or more GPR common mid-point
320 surveys to estimate EM wave velocity along the peat column and convert two-way travel time
321 into depth for common offset profiles; 3) one or more electrical resistivity transects between 48-
322 144 m long to provide additional information related to: a) peat thickness in regions where GPR
323 was anticipated to fail due to thicknesses being greater than the GPR penetration depth and/or
324 excessive GPR attenuation associated with high electrical conductivity; and b) variations in the
325 lithology of the sub-peat mineral deposits; and 4) one or more direct soil cores in order to
326 confirm depth of the peat-mineral soil interface and to obtain samples for subsequent C analysis
327 at selected locations. Since not every core collected was analyzed for C content, Table 2 presents
328 a summary of cores collected including average C percent and content along the peat column.

329

330 **4.3. Results**

331 ~~3 — A set of geophysical surveys combined with direct sampling was conducted at each study~~
332 ~~site and consisted of: 1) one or more GPR common offset transects between 30-100 m long to~~
333 ~~identify the peat-mineral soil reflector and other stratigraphic features (such as presence of wood~~
334 ~~layers or buried buttressed trees) within the peat soil reflection record; 2) one or more GPR~~

335 common mid-point surveys to estimate EM wave velocity along the peat column and convert
336 two-way travel time into depth for common offset profiles; 3) one or more electrical resistivity
337 transects between 48-144 m long to provide additional information related to: a) peat thickness in
338 regions where GPR was anticipated to fail due to thicknesses being greater than the GPR
339 penetration depth and/or excessive GPR attenuation associated with high electrical conductivity;
340 and b) variations in the lithology of the sub-peat mineral deposits; and 4) one or more direct soil
341 cores in order to confirm depth of the peat-mineral soil interface and to obtain samples for
342 subsequent C analysis at selected locations. Since not every core collected was analyzed for C
343 content, Table 2 presents a summary of cores collected including average C percent and content
344 along the peat column. Specific results per site are explained below.

345

346 **4.1.1 Tanjung Gunung: shallow peat (0-4 m)**

347 _____ A set of two orthogonal common-offset profiles were collected at Site TG1 with
348 the 0 m distance in Line 1 (Figure 2a) crossing Line 2 (Figure 2b) at 24 m along the profile. An
349 average EM wave velocity of 0.04 m ns^{-1} for the peat column was estimated from GPR common
350 mid-point profiles (not shown here for brevity). Using this velocity estimate, GPR common
351 offset profiles (Figure 2) identified a 4 m thick peat column that is laterally continuous over the
352 profile.

353 Direct coring at two locations (shown in Figure 2a and 2b respectively) confirms a total peat
354 thickness of 4 m with a 0.1-0.2 m sandy clay transition (also containing some organics) into a
355 clayey mineral soil at about 4.2 m depth. Direct coring also detected the presence of: 1) a water
356 table at 0.5 m depth coinciding with the presence of a distinctive reflector in the GPR record
357 (particularly clear in Figure 2b); 2) a woody area between 2-3 m depth (indicated in Figure 2)
358 resulting in isolated points of core refusal that coincide with the presence of hyperbolic

359 | diffractions in the reflection record. Extracted core samples showed an average of 58.5 % C and
360 | C content of 2,311.0 Mg ha⁻¹ (Table 2).

361 | Electrical resistivity imaging results for Line 1 and Line 2 at Site TG1 are shown in
362 | Figure 3a and 3b respectively. Direct cores as shown in Figure 2 are superimposed for
363 | comparison. The resistivity inversion shows a relatively conductive (resistivity less than 100
364 | Ohm m) upper layer, underlain by a more resistive unit of undetermined thickness. The upper
365 | layer (showing a progressive increase in resistivity with depth between 60-200 Ohm m)
366 | correlates with the terrestrial peat deposit as confirmed from direct sampling and GPR.
367 | ~~Resistivity values for the upper layer are comparable with values obtained in northern peatlands~~
368 | ~~and partly attributed to the low ionic concentration of the peat pore water (Slater and Reeve~~
369 | ~~2002, Comas et al. 2011).~~ The underlying resistive layer (ranging between 200-300 Ohm m)
370 | includes both a transition layer composed of a mixture of sand and clay (with some organics) and
371 | a clayey mineral soil as confirmed from coring. Although lower ~~resistivities~~resistivities are
372 | typical for clayey mineral sediments that are usually found below peat, in this case the higher
373 | resistivities are attributed to a sandy mineral soil matrix as confirmed from coring in the
374 | transition layer. ~~Sandy mineral soils below the organic sediments of other peatlands in Central~~
375 | ~~Kalimantan have been reported (Shimada et al. 2001).~~

376 | GPR common offset profiles at Site TG2 (Figure 4 and 5) identified a variable peat
377 | column ranging between 0.1-3.4 m along the profiles. An average EM wave velocity of 0.038 m
378 | ns⁻¹ for the peat column (slightly lower than that at TG1) was estimated from GPR common mid-
379 | point profiles. As shown in the reflection record in Figure 4a and confirmed with direct coring,
380 | the reflector interpreted as the peat-mineral soil interface deepens from the surface (at 70 m
381 | along the profile where the reflector is not discernible from the ground coupling) to 1.5 m (at 74
382 | m along the profile) towards the NE, representing a total increase of 1.4 m in peat thickness over

383 a 4 m horizontal distance (i.e. between 70 and 74 m along the profile). This trend extends to the
384 end of the profile where the peat-mineral soil exceeds depths of 3 m, where peat thickness
385 increases by over 3 m in about 20 m along the transect. The ERI images are consistent with this
386 interpretation (Figure 4b) depicting a resistive upper layer (100-370 Ohm m interpreted as peat)
387 underlain by a conductive unit (as low as 20 Ohm m) interpreted as clay and confirmed from
388 both coring and surface outcrops between 0 and 60 m along the transect. Figure 5a represents the
389 continuation of the GPR common offset profile in Figure 4a towards the NE. In this case peat
390 thickness is almost uniform (as confirmed with coring and depicted in Figure 5a), with peat
391 thickness changing only by 0.4 m across the 100 m long profile. This profile also confirms the
392 presence of a distinctive reflector at about 0.8 m depth interpreted as the water table as
393 confirmed from coring. Although the coring did not explicitly detect points of core refusal (like
394 those at TG1), the GPR record also shows the presence of hyperbolic diffractions in the
395 reflection record (i.e. between 40-85 m along the transect and between 2-3 m depth in Figure 5a
396 as indicated by white arrows). The ERI image in Figure 5b follows the GPR profile in Figure 5a
397 and is consistent with the results shown in Figure 4b depicting a resistive upper layer (100-370
398 Ohm m interpreted as peat) underlain by a conductive unit (as low as 20 Ohm m) interpreted as
399 clay. For TG1.1-TG1.3, the organic soil had an average C percent of 49.3 % C and C content of
400 1,683.4 Mg ha⁻¹ (Table 2).

401

402 **4.3.2. Pelang Forest: intermediate and deep peat (5-9 m)**

403 Geophysical surveys constrained with direct coring at Pelang Forest contrast with those
404 previously described at Tanjung Gunung by showing greater peat thicknesses ranging between 5
405 m at Site P1 up to 9 m at Site P2. GPR and electrical resistivity surveys at Site P1 were collected
406 at different locations separated by about 1 km since GPR transects at this site were not accessible

407 with heavy resistivity instrumentation. Similar to Site TG1, an average EM wave velocity of 0.04
408 m ns⁻¹ for the peat column was estimated from GPR common mid-point profiles at this site. GPR
409 common offset profiles at Site P1 (Figure 6) show a reflection record characterized by: 1) a depth
410 of penetration of 5 m followed by signal attenuation that coincides with a sandy clay transition
411 (with some organics) between 5-7.5 m underlain by a clayey mineral soil as confirmed from
412 coring (shown at 95 m along the profile in Figure 6); 2) a distinct reflector at about 35-40 ns
413 interpreted as the water table; 3) a sequence of laterally discontinuous chaotic reflectors with
414 some hyperbolic diffractions (i.e. as seen at 150 ns and 15 m along the profile and indicated by a
415 small white arrow); and 4) a possible depression feature within the peat column between 150-250
416 ns and 10-35 m along the profile, with a SE side tilting about 9 degrees towards the NW and a
417 NW side tilting about 13 degrees towards the SE. The white arrow in Figure 6 indicates the
418 lowest point of this feature. ~~It is important to consider that although migration has not been
419 included in any GPR common offset in order to preserve the appearance of diffractions,
420 application of a 1D Stolt migration in the common offset in Figure 6 (based on a velocity of 0.04
421 m ns⁻¹) resulted in changes in the tilt of the reflectors of less than one degree.~~

422 Electrical resistivity imaging results at Site P1 (Figure 7) show an interface at about 5 m
423 depth (as confirmed from coring) between an upper resistive layer with a resistivity ranging
424 between 150-300 Ohm m interpreted as peat, underlain by a conductive unit (as low as 30 Ohm
425 m) interpreted as clay and confirmed from coring. These resistivity values are consistent with
426 those previously shown for Site TG2 in Figure 4b. Although boundaries are not clear, a
427 transitional layer along the column between the peat and clay units shows intermediate resistivity
428 values (around 100 Ohm m) and is coincident with the mixture of sand, clay and organics with a
429 thickness of about 2.5 m identified in the coring. Although not directly confirmed from coring, it
430 appears the interface between the peat and the sandy clay is variable across the profile in Figure

431 | 7, indicating an undulating peat thicknesses between 5 m (i.e. at core location at 22 m along the
432 | line, and at 70, 105, or 120 m along the line based on ERI alone) and 7.5-8 m (i.e. at 12, 90, or
433 | 130 m along the profile). The ERI profile also shows a strong lateral resistivity variation in the
434 | resistivity of the deeper mineral soil (i.e. below 10 m depth) varying between 30-100 Ohm m
435 | from the SE to the NW direction. Cores P1.1 and P1.2 averaged 50.8 % C with a C content of
436 | 2,677.1 Mg ha⁻¹ (Table 2).

437 | Variability in peat thickness at Site P2 (Figure 8) is similar to that described for Site P1
438 | (Figure 7) and is confirmed at three coring locations (at 10, 50 and 100 m along the profile)
439 | resulting in total peat thicknesses of 9 m or more , 8.7 and 8.8 m respectively. Since topography
440 | can be considered flat at the scale of measurement used in this profile, these results confirm that
441 | the interface between the peat and the underlying sandy clay transition is undulating and that
442 | resistivity values for the peat (between 100-185 Ohm m) and transitional layer (below 100 Ohm
443 | m) are consistent with those shown in Figure 7. The clay layer imaged with the resistivity profile
444 | in Figure 7 (and confirmed from coring in that figure) is also visible in Figure 8 just below the
445 | transitional layer and at approximate depths between 10-14 m. ~~Although GPR profiling at this
446 | site was also performed using 100 MHz antennas, results are inconclusive (and thus not
447 | presented here) since subsurface reflections appear to only penetrate about 3-4 m depth. Site P2
448 | was surveyed during the last day of the field campaign when 50 MHz antennas malfunctioned as
449 | explained in the methods section.~~ For cores P2.1 and P2.2 the soils averaged 57.0 % C with a C
450 | content of 5,892.3 Mg ha⁻¹ (Table 2).

451

452 | **5.4. Discussion**

453 | **5.4.1. Peat thickness**

454 | ~~In general, pAs related to the first objective of this paper (i.e. peat thickness estimates using GPR~~
455 | ~~and ERI were consistent across sites ion using geophysical methods). Estimated peat thicknesses~~
456 | ~~are generally the results presented here are consistent between the measurement methods,~~
457 | although several differences ~~between methodologies need to be considered~~ are noted. GPR ~~is-was~~
458 | particularly ~~useful-effective~~ for characterizing peat thickness for shallow peat columns (i.e. TG1
459 | and TG2 in Figures 2 and 5b respectively) and ~~is~~-able to quantify depth of the peat-mineral soil
460 | interface at ~~em~~centimeter scale resolution both vertically and laterally from a strong reflector that
461 | ~~matches-matched~~ closely with coring results. This reflector resembles the peat-mineral soil
462 | interface as typically detected with GPR in boreal peatlands in North America and Europe,
463 | exemplified in several studies for those higher latitude systems (Warner et al. 1990, Jol and
464 | Smith 1995, Slater and Reeve 2002, Parsekian et al. 2012, Comas et al. 2013). However, the
465 | GPR method, ~~as-as based on the used with~~ antenna frequencies ~~used-available~~ for this study,
466 | ~~shows limitations was limited~~ for imaging deep (i.e. 9 m or more) peat columns (i.e. Sites P1 and
467 | P2) ~~in this study~~. We attribute these limitations to: 1) thicker peat columns that excessively
468 | attenuate the GPR signal, and/or 2) attenuation due to the presence of clay-rich transition layers
469 | with high electrical conductivities as depicted by the low resistivity values in P1 and P2 (Figures
470 | 7 and 8). Attenuation in clay-rich areas was to be expected since it is well known than the
471 | effectiveness of GPR in peatlands is compromised when electrical conductivity of peat is high
472 | due to high electrical fluid conduction or high percent of clay ~~fractions~~ (Theimer et al. 1994).
473 | _____ Electrical resistivity imaging also proves useful for detecting changes in ~~the~~-peat
474 | thickness ~~column~~-across ~~the different~~-sites and for estimating the ~~depth of~~ interface between peat
475 | and mineral soil. When compared to GPR, electrical resistivity shows similar imaging
476 | capabilities for estimating both shallow and deep peat columns in the study areas (due to larger
477 | depths of investigation), ~~however-although~~ resolution (both vertical and lateral) is ~~more~~

478 | ~~limited~~lower than that of GPR results, particularly as depth increases. The boundaries between
479 | the resistive top layer corresponding to the peat and the underlying conductive materials
480 | corresponding to the clay and transitional layer are not clear and are depicted by a gradual
481 | increase in conductivity (i.e. Figure 4b, 7, and 8). These results are consistent with previous
482 | studies in northern peatlands which demonstrate that electrical conductivity is not an accurate
483 | indicator of peat thickness when peat is underlain by a conductive layer ~~due to the increase in~~
484 | ~~specific conductance of peat pore fluid towards the base of peat and the effect of the mineral soil~~
485 | (Slater and Reeve 2002). The results presented here also confirm the same issue when peat is
486 | underlain by a resistive material (Figure 3-), ~~which is not uncommon in Indonesia. For~~
487 | ~~example. Sandy mineral soils below the organic sediments of other peatlands in Central~~
488 | ~~Kalimantan have been reported (Shimada et al. 2001).~~ Despite these limitations, a good
489 | correspondence exists between the limit of the uppermost high resistivity values at sites TG2, P1
490 | and P2 (depicted in red and orange in Figures 4b, 7, and 8) and the peat layer interface.

491 | ~~Although GPR and ERI datasets presented in this work here are limited particularly in~~
492 | ~~terms of areal extent and scale of measurement, our intent here was to test and demonstrate the~~
493 | ~~potential of the methods for estimating peat thickness in tropical peatlands at better resolution~~
494 | ~~than traditional methods (i.e. coring). Therefore, Since (For that reason geophysical surveys were~~
495 | ~~developed at plot level scales averaging 100 m long profiles in this study wwith the aim of~~
496 | ~~upsampling measurements in subsequent studies. Furthermore,~~ the ultimate aim of this work is to
497 | increase the accuracy of peat C storage estimates ~~by using methods able to quantify peat~~
498 | ~~thickness at high lateral resolution (i.e. reaching cm for GPR) when compared to traditional~~
499 | ~~coring. It is important to consider that GPR or ERI as applied here detects interfaces representing~~
500 | ~~contrasts in physical properties- which can be used to obtain highly accurate estimates of peat~~
501 | ~~volume. When combined with sampling of representative peat soils (for example C content), but~~

502 ~~it is not able to directly quantify C content. For that reason geophysical surveys are combined~~
503 ~~with direct sampling of soils and for C density determination, total peat carbon storage estimates~~
504 ~~can be largely improved at the site level or project level C content analysis in the laboratory. we~~
505 ~~consider how geophysical methods may compare to traditional coring methods for estimating~~
506 ~~carbon stocks. Although the GPR datasets presented in this work are limited particularly in terms~~
507 ~~of areal extent and scale of measurement, our intent here is to exemplify the potential of the~~
508 ~~method for enhancing our ability to measure peat thickness and better develop C stock~~
509 ~~estimates.~~

510 4.2. Peat C stocks

511 _____ The profile from Site TG-2 in Figure 5 can be used to investigate how subtle changes in
512 peat thickness ~~as detected from GPR~~ (representing a maximum gradient below 0.02 deg) may
513 influence overall peat ~~and C~~ carbon stock estimates. Figure 9 shows a comparison between a) peat
514 thickness estimated from GPR at a total of 539 locations (or every 0.2 m along the profile ~~shown~~
515 in Figure 5a); and direct coring at 5 locations (or approximately every 20 m along the profile)
516 (Figure 9a); and b) peat thickness estimated from ERI at a total of 190 locations (interface shown
517 in Figure 5b); and direct coring at 5 locations (Figure 9b). ~~Although the regularization constraint~~
518 ~~used in the ERI inversion procedure has the effect of smoothing structural boundaries, the depth~~
519 ~~to such boundaries can be estimated in a semi-quantitative way when some kind of ancillary~~
520 ~~information is available to calibrate the definition of these interfaces. Thus, the lower peat~~
521 ~~boundary was ‘picked’ from the ERI image using the average inverted resistivity value at pixels~~
522 ~~corresponding to the interface identified from coring (mean = 131 Ohm m, standard deviation =~~
523 ~~17 Ohm m). At each of the 190 horizontal locations, the interface was picked as the vertical~~
524 ~~location below 1.5 m depth (to ensure picking below the near surface resistivity transition~~
525 ~~probably resulting from a change from disturbed to undisturbed peat) where the inverted~~

526 ~~resistivity most closely matched the estimated interface resistivity value. ERI estimates do not~~
527 ~~consider the first and last 5 meters along the profile due to the low resolution in the inversion.~~
528 GPR estimates in Figure 9a are based on an average velocity of 0.038 m ns⁻¹ ~~(or a constant~~
529 ~~relative dielectric permittivity)~~ for the entire peat column. ~~Although EM wave velocity in peat~~
530 ~~soils most typically range between 0.036-0.044 m ns⁻¹ (Parsekian et al. 2012) our average was as~~
531 ~~determined from 1) the reflector corresponding to the peat-mineral soil interface in GPR 1)~~
532 common midpoint surveys ~~(consistently showing values of 0.038 m ns⁻¹ at two different locations~~
533 ~~at TG2 and using two different antenna frequencies (i.e. 100 and 200 MHz),)~~; and 2) the travel
534 time recorded at the 5 coring locations (consistently showing estimates 0.038 ± 0.001 m ns⁻¹);
535 ~~thus representing a true velocity average of the peat column. The lower peat boundary was~~
536 ~~picked~~ selected from the ERI image using the average inverted resistivity value at pixels
537 ~~corresponding to the interface identified from coring (mean = 131 Ohm-m, standard deviation =~~
538 ~~17 Ohm-m). Lateral variability in depth to the mineral soil at TG2 ranges between 2.9-3.4 from~~
539 ~~the GPR and 2.4-3.7 m along the same transect at TG2 as estimated from the ERI images (Figure~~
540 ~~5b-9a and 9b respectively), confirming (despite the more limited vertical resolution when~~
541 ~~compared to GPR, as expected)~~ that substrate topography is highly variable laterally. These
542 results also confirm previous studies showing lateral variability in mineral substrate topography
543 across several peat domes in Borneo (Dommain et al. (2010) after Konsultant (1998)).
544 ~~Furthermore, these results confirm, as expected, that vertical resolution of peat profiles obtained~~
545 ~~from ERI is more limited when lower than those obtained using compared to GPR, as expected.~~

546 Error bars in the GPR data (± 0.05 m average in Figure 9a) were calculated from the
547 difference in peat thickness between GPR using this average velocity and that measured from the
548 coring. Error bars in the ERI data (Figure 9b) were computed as the maximum misfit at each
549 horizontal location between (1) the interpolated interface depth taken from coring and (2) the

550 ERI estimated interface depth using the mean resistivity value ± 2 standard deviations. Assuming
551 that lateral variability in peat thickness between cores is non-existent when the same thickness is
552 estimated for contiguous cores (i.e. perfectly horizontal interface), and that thickness increases
553 gradually with distance (i.e. constant gradient) as shown in the shaded areas in Figure 9a, the
554 overall peat surface area for the profile is estimated to be 324 m². Thickness estimated from
555 individual GPR traces (every 0.2 m), produces an overall peat surface area of 331 m², an increase
556 of 2.1 %. The difference in surface area represents a total increase of 1,171 kg of C along the two
557 dimensional profile if we assume a C content of 1,673.1 Mg C ha⁻¹ as averaged for the peat
558 column in Core TG2.1-TG2.3 (Table 2). Due to the limitations in terms of a) vertical resolution,
559 and b) lateral extent of the profile (i.e. low inversion results on the edges of the profiles) a similar
560 approach using ERI peat thickness estimates is more uncertain and therefore is not included here.
561 Variability in peat thickness was only 2.9-3.4 m (estimated from GPR traces) or 0.4-0.5 m over
562 the 100 m TG2 transect. Although the 7 m² difference in surface area between GPR and coring
563 measurements represents only 0.07 m in average peat thickness, when scaled ~~per~~
564 ~~areavolumetrically~~ the difference between GPR and coring estimates is 37 MgC/ha, which
565 illustrates how relatively small differences in depth estimates can impact overall C storage
566 calculations. Since most peat formations in Indonesia occur at much larger spatial scales (i.e.
567 tens of kilometers or more), GPR surveys over broader areas are shown here to be capable of
568 largely reducing uncertainties regarding peat thickness and C storage. Moreover, as peat C
569 density in tropical peat soils becomes better constrained (Rodríguez et al. 2013), local to regional
570 estimates of peat C storage could be improved through the use of GPR methods to accurately
571 determine peat thickness. Considering peat thickness can also change ~~more~~ dramatically over
572 short distances depending on geomorphic setting (e.g.. about 1.5 m difference in peat thickness
573 within only 4 m along the Site TG-2 profile in Figure 4), measuring peat thickness at finer spatial

574 resolution would thus significantly improve current C stock estimates. ~~For example other~~
575 ~~authors have also estimated uncertainties in C storage between 13–25 % due to unconformities of~~
576 ~~the underlying mineral soil in several peat domes in Central Kalimantan (Jaenicke et al. 2008).~~
577 ~~More accurate estimates of peat thickness are clearly required to properly define C stocks in~~
578 ~~Indonesia and likely other tropical peatlands.~~

579 **4.3. Peat formation**

580 ~~As related to the second objective of this paper (i.e. interpretation of geological settings from our~~
581 ~~geophysical data). The results presented in this work here also demonstrate show potential for~~
582 ~~using GPR and ERI methods to improve improving the~~ understanding of processes associated
583 with peatland formation ~~as reflected in the differences in geophysical signatures when comparing~~
584 ~~the two study sites (TG and P). Differences in the GPR reflection record and contrasts in~~
585 ~~electrical conductivity between the two study sites (TG and P) are here interpreted as differences~~
586 ~~in peat ecosystem type and developmental history between sites.~~ First, there is a sharp difference
587 between the profiles at TG1 and TG2, as the resistivity profile increases with depth at TG1 (i.e.
588 higher resistivity at the bottom of the profile, Figure 3) whereas it decreases at TG2 (i.e. lower
589 resistivity at the bottom of the profile, Figure 3). Second, the interface between peat-mineral soil
590 at TG1 and TG2 is characterized by a set of 2-3 sharp reflectors in the GPR record (i.e. Figure 2,
591 4, and 5), that is absent at Site P where reflectors are sharply attenuated when reaching depths
592 corresponding to the transition zone between peat and clay. Third, resistivity results do not show
593 marked differences in terms of electrical conductivity between sites along the peat-clay interface,
594 although coring results show a marked increase in thickness of the transition zone (mostly
595 corresponding to mixtures of clay and sand) with averages between 0.1-0.2 m for Sites TG1 and
596 TG2 and averages reaching 2.5 m for Site P1. These differences may be attributed to two related
597 issues: 1) the developmental history of peatland initiation and formation at each specific site; and

598 2) the differences in site location as related to physiographic type of terrain and the
599 characteristics of peat ecosystems at each site. As shown in Figure 1, sites TG1 and TG2
600 correspond to MDW or shallow peat swamp ecosystems while sites P1 and P2 are characterized
601 by GBT or large ombrotrophic peat swamp ecosystems. Coastal peat swamps in Kalimantan
602 have been described as the result of peat accumulation developed on marine clay and mangrove
603 deposits of river deltas and coastal plains during the ~~mid-late~~ Holocene (~~~7,000~~-5,000 cal BP)
604 (Supiandi 1988, Dommain et al. 2011). As sea levels fell around 5,000 cal BP, sandy beach
605 ridges were exposed and directly colonized by peat swamps and mud flats were covered by
606 mangroves (Cameron et al. 1989, Dommain et al. 2011, Dommain et al. 2014). While sites at TG
607 may be related to peat swamp colonization over sandy ridges (as reflected by the presence of a
608 highly resistive mineral soil at TG1 and/or a thin transitional layer at both TG1 and TG2), sites at
609 P may be characterized by colonization of mud flats and mangrove deposits (as characterized by
610 much thicker organomineral mixing horizons and potential increased electrical conductivity that
611 results in a marked attenuation in the GPR reflection record, i.e. Figure 6). Furthermore, the ERI
612 profiles also show lateral variation in resistivity associated with variability in the topography of
613 the deeper mineral soil and associated with peat thickness (i.e. Figure 5b and 9b). Local
614 depressions can be also identified in Figure 7 (i.e. around 80-100 m distance along the profile)
615 and suggest that peat soil undulates at a fine scale. Similar features can also found in Figure 8
616 (i.e. between 20-50 m distance along the profile).

617 **4.4 Peat matrix** — ~~Also as related to the second objective (inferring information about peat~~
618 ~~composition from our geophysical data). Differences in geophysical signatures may also be~~
619 ~~supported by the difference in C content shown for each specific site as C content (analyzed~~
620 ~~from core samples in the laboratory for each site is very consistent between cores (Table 2).~~
621 ~~However, sharp differences exist when comparing sites, showing values (in terms of Mg C ha⁻¹)~~

622 at P2 that are twofold the averages in P1 or TG1 and threefold the averages in TG2. Such
623 increases correspond to peat thickness depicting higher C contents for thicker peat columns (e.g.
624 Site P2) and lower C contents for thinner peat columns (e.g. Site TG2). This also appears to be
625 related to type of peat ecosystem as depicted in Table 1, which suggest higher C contents in deep
626 (rather than shallow) peat swamps. The relation between C content variability and peatland type
627 is also supported by previous studies in the region. For example, Shimada et al (2001) concluded
628 that peatland type was the most important factor controlling volumetric C density in peatlands of
629 Central Kalimantan mainly due to variability in physical consolidation (mainly porosity) from
630 peat decomposition or nutrient inputs. They also suggested that the those peat soils showing less
631 frequent woody layers (typically corresponding to terrace peat) are more decomposed (i.e. lower
632 porosity) and therefore show higher volumetric C density. Our geophysical results seem to
633 confirm this hypothesis by showing a larger presence of interpreted woody layers in the GPR
634 record along those soils with lower C content values (i.e. TG sites), while P sites (with higher C
635 contents) do not seem to identify a clear presence of wood layers in the GPR record. Site level
636 disturbance and land use history may also contribute substantially to C content of the surface
637 peat, as peat burning, profile mixing, and sedimentation from tailings of canal construction could
638 affect C content.

639 _____
640 Finally, the spatial resolution provided by GPR common offset profiles also shows the potential
641 for better understanding the nature and internal structure of the peat matrix. For example,
642 referring to the presence of hyperbolic diffractions in the GPR record, Figures 2a, 2b, and 5 show
643 the presence of several areas with a high density of diffractions. These diffractions are
644 particularly abundant in Figure 2a between 10-20 m distance along the profile and at 2.5-3 m
645 depth, or in Figure 5 between 70-85 m distance along the profile and between 2-3 m depth (white

646 arrows in Figure 5). Diffractions are associated with the presence of objects that may act as
647 isolated reflector points such as cobbles and boulders (Neal 2004). In this case, we associate
648 hyperbolic diffractions in GPR common offsets to the presence of buried woody debris (as
649 further confirmed through coring). Other investigations in northern peatlands have also related
650 GPR diffractions to the presence of wood (Slater and Reeve 2002). Such features are absent at
651 P1 (Figure 6) where more laterally continuous reflections (i.e. at 3, 4, and 4.5 m depth between
652 40 to 90 m along the profile) are present. Previous studies in Kalimantan region have also
653 consistently shown layers with large quantities of undecomposed woody fragments
654 heterogeneously distributed within the peat column (Shimada et al. 2001). Furthermore, some of
655 these laterally continuous reflectors generate a depressional feature between 10 to 30 m along the
656 profile of P1 (center point indicated by a white arrow in Figure 6) as depicted by a sharp reflector
657 at depths between 3.5 to almost 6 m that tilts 13 and 9 degrees respectively on the NW and SE
658 sides of the profile. Although not directly confirmed in the field through direct coring, this
659 feature might be related to the presence of buttressed trees which often prompt the formation of
660 hummocks and water ponding upslope (Dommain et al, 2010), or the uprooting of such trees due
661 to wind and the formation of depressional features as the root zone is displaced. Alternatively,
662 these feature may also be associated to the infill process in a tip-up pool. As described by
663 Dommain et al. (2015) for peatlands in Borneo tip-up pools are commonly formed when
664 lightning strikes a tree inducing its fall and generating a discontinuity in the peat deposit and a
665 pool subsequently infilled with younger material. Because horizontal reflectors seem to overlap
666 the tilting reflectors may support the hypothesis that the depression formed suddenly, to be later
667 filled up progressively with ~~more~~ younger peat. Although this may represent an isolated feature
668 in our dataset Dommain et al. (2015) have recently demonstrated the importance of such features

669 | when describing carbon accumulation rates and how it may complicate paleo-environmental
670 | reconstructions.

671

672 | **56. Conclusions**

673 | ~~This study~~ ~~This study has demonstrated~~ the ~~potential of~~ feasibility of using GPR and ERI
674 | ~~imaging~~ for non-invasively mapping ~~of the~~ subsurface of peatlands in Indonesia, at a spatial
675 | resolution previously unreported in tropical peatland systems which are traditionally
676 | ~~assessed/measured~~ using coring methods. ~~Specifically this~~ The results presented study highlights
677 | the opportunity to use the reflection record from GPR to improve peat thickness estimates while
678 | providing information on certain attributes of the peat matrix such as presence of wood layers or
679 | buttressed trees, or peat soil nature as related to origins related to peatland ecosystem type (i.e.
680 | mangrove vs. freshwater peat). While in general GPR is able to predict peat thickness with cm
681 | resolution the method shows some limitations emerged (i.e. signal attenuation) for peat
682 | columns exceeding 5 m thick. Although the vertical resolution of ERI is more limited, peat
683 | thickness determination shows comparable results for either shallow or deep peat columns. A
684 | comparison between peat thickness estimates from GPR, ERI and coring showed a variability
685 | exceeding 2 % in peat surface area (or 1,191 kg of C assuming C contents of 170 kg C m⁻² as
686 | averaged from core samples), although this was based on a short 100 m two dimensional profile
687 | ~~showing/indicating~~ changes in thickness of less than 0.5 m. Such discrepancies may be larger
688 | when considering transects with a more variable peat thickness (such as those here showing up to
689 | 1.5 m vertical difference over only 4 m in the horizontal). Given the difficulty of capturing such
690 | variability with traditional methods (such as coring), estimating total current C stocks in
691 | Indonesian peatlands at local scales should be revisited using methods such as GPR or electrical
692 | resistivity imaging that better account for lateral variability.

693

694 **67. Acknowledgements**

695 This work was supported by the U.S. Agency for International Development (USAID).
696 We are indebted to Kent Elliot (U.S. Forest Service) for all his help with logistics and fieldwork
697 during this study. We are also thankful to Sofyan Kurnianto (CIFOR/Oregon State University)
698 and Ophelia Wang (USAID-IFACS) for their help in the field, and to all the local Indonesians
699 and helpers involved in this research for their support at the study sites. We thank R. Dommain
700 for helpful discussions and revisions in ~~some of~~ the materials presented in this study. We also
701 thank four anonymous reviewers and the Editor for helpful comments to improve an earlier
702 version of this manuscript.

703

704 **78. References**

705 Binley, A. and A. Kemna. 2005. DC Resistivity and Induced Polarization Methods. *in* Y. Rubin
706 and S. S. Hubbard, editors. Hydrogeophysics. Springer, New York.
707 Cameron, C.C., J.S. Esterle, and A.P. Curtis. 1989. The geology, botany and chemistry of
708 selected peat-forming environments from temperate and tropical latitudes. International
709 Journal of Coal Geology **12**:105-156.
710 Comas, X. and L. Slater. 2007. Evolution of biogenic gasses in peat blocks inferred from non-
711 invasive dielectric permittivity measurements. Water Resources Research **43**:W05424.
712 Comas, X. , L. Slater, and A. Reeve. 2004. Geophysical evidence for peat basin morphology and
713 stratigraphic controls on vegetation observed in a Northern Peatland. Journal of
714 Hydrology **295**:173-184.
715 Comas, X., N. Kettridge, A. Binley, L. Slater, A. Parsekian, A. J. Baird, M. Strack, and J. M.
716 Waddington. 2013. The effect of peat structure on the spatial distribution of biogenic
717 gases within bogs. Hydrological Processes:doi: 10.1002/hyp.10056.
718 Comas, Xavier, Lee Slater, and A. S. Reeve. 2011. Pool patterning in a northern peatland:
719 Geophysical evidence for the role of postglacial landforms. Journal of Hydrology
720 **399**:173-184.
721 Dommain, R., J. Couwenberg, and H. Joosten. 2010. Hydrological self-regulation of domed
722 peatlands in south-east Asia and consequences for conservation and restoration. Mires
723 and Peat **6**.
724 Dommain, R., J. Couwenberg, P. H. Glaser, H. Joosten, I. Nyoman, and N. Suryaputra. 2014.
725 Carbon storage and release in Indonesian peatlands since the last deglaciation.
726 Quarternary Science Reviews **97**:1-32.

Formatted: Font: (Default) Times New Roman, 12 pt

727 Dommain, René, Alexander R. Cobb, Hans Joosten, Paul H. Glaser, Amy F. L. Chua, Laure
728 Gandois, Fuu-Ming Kai, Anders Noren, Kamariah A. Salim, N. Salihah H. Su'ut, and
729 Charles F. Harvey. 2015. Forest dynamics and tip-up pools drive pulses of high carbon
730 accumulation rates in a tropical peat dome in Borneo (Southeast Asia). *Journal of*
731 *Geophysical Research: Biogeosciences*:2014JG002796.

732 Dommain, René, John Couwenberg, and Hans Joosten. 2011. Development and carbon
733 sequestration of tropical peat domes in south-east Asia: links to post-glacial sea-level
734 changes and Holocene climate variability. *Quaternary Science Reviews* **30**:999-1010.

735 Geuzaine, C. and J.F. Remacle. 2009. Gmsh: a three-dimensional finite element mesh generator
736 with built-in pre- and post-processing facilities. *International Journal for Numerical*
737 *Methods in Engineering* **79**:1309-1331.

738 Hooijer, A., M. Silvius, H. Woesten, and S. Page. 2006. Peat- CO₂: Assessment of CO₂
739 emissions from drained peatlands in SE Asia; Delft Hydraulics report Q3943.

740 Jaenicke, J., J. O. Rieley, C. Mott, P. Kimman, and F. Siegert. 2008. Determination of the
741 amount of carbon stored in Indonesian peatlands. *Geoderma* **147**:151-158.

742 Jol, H. M. and D. G. Smith. 1995. Ground penetrating radar surveys of peatlands for oilfield
743 pipelines in Canada. *Journal of Applied Geophysics* **34**:109-123.

744 Joosten, H. 2009. *The Global Peatland CO₂ Picture*. Ede.

745 Konsultant, PS. 1998. *Detailed Design and Construction Supervision of Flood Protection and*
746 *Drainage Facilities for Balingian RGC Agricultural Development Project, Sibul Division,*
747 *Sarawak (Inception Report)*. Kuching.

748 Menke, W. 1989. *Geophysical Data Analysis: Discrete Inverse Theory*. Academic. Press, Inc.,
749 New York.

750 Meyer, J.H. 1989. Investigation of Holocene organic sediments: a geophysical approach.
751 *International Peat Journal* **3**:45-57.

752 Neal, A. 2004. Ground-penetrating radar and its use in sedimentology: principles, problems and
753 progress. *Earth-Science Reviews* **66**:261-330.

754 Page, S. E., J. O. Rieley, and C. J. Banks. 2011. Global and regional importance of the tropical
755 peatland carbon pool. *Global Change Biology* **17**:798-818.

756 Page, Susan E., Florian Siegert, John O. Rieley, Hans-Dieter V. Boehm, Adi Jaya, and Suwido
757 Limin. 2002. The amount of carbon released from peat and forest fires in Indonesia
758 during 1997. *Nature* **420**:61-65.

759 Parry, L. E., L. J. West, J. Holden, and P. J. Chapman. 2014. Evaluating approaches for
760 estimating peat depth. *Journal of Geophysical Research: Biogeosciences*
761 **119**:2013JG002411.

762 Parsekian, A. D., L. Slater, S. D. Sebestyen, R. K. Kolka, D. Ntarlagiannis, J. Nolan, and P.
763 Hanson. 2012. Comparison of uncertainty in peat volume and soil carbon estimated using
764 GPR and probing. *Soil Science Society of America Journal* **76**:1911-1918.

765 RePPProT. 1990. *Regional Physical Planning Programme for Transmigration. The land*
766 *resources of Indonesia: a national overview. Main report*. Ministry of Transmigration and
767 *Land Resources Department/Bina Program., Jakarta*.

768 Ritung, S., Wahyunto, K. Nugroho, Sukarman, Hikmatullah, Suparto, and C. Tafakresnanto.
769 2011. *Peta Lahan Gambut Indonesia Skala 1:250.000 (Indonesian peatland map at the*
770 *scale 1:250,000)* Indonesian Center for Agricultural Land Resources Research and
771 *Development, Bogor, Indonesia*.

772 Rodríguez, V., F. Gutiérrez, A.G. Green, D. Carbonel, H. Horstmeyer, and C. Schmelzbach.
773 2013. Characterising saging and collapse sinkholes in a mantled karst by means of
774 Ground Penetrating Radar (GPR). *Environmental and Engineering Geoscience* **In Press**.
775 Rosa, E., M. Larocque, S. Pellerin, S. Gagné, and B. Fournier. 2009. Determining the number of
776 manual measurements required to improve peat thickness estimations by ground
777 penetrating radar. *Earth Surface Processes and Landforms* **34**:377-383.
778 Shimada, Sawahiko, Hidenori Takahashi, Akira Haraguchi, and Masami Kaneko. 2001. The
779 carbon content characteristics of tropical peats in Central Kalimantan, Indonesia:
780 Estimating their spatial variability in density. *Biogeochemistry* **53**:249-267.
781 Slater, L. and A. Reeve. 2002. Understanding peatland hydrology and stratigraphy using
782 integrated electrical geophysics. *Geophysics* **67**:365-378.
783 Supiandi, S. 1988. Studies on peat in the coastal plains of Sumatra and Borneo. Part I:
784 Physiography and geomorphology of the coastal plains. *Southeast Asian Studies* **26**:308-
785 335.
786 Theimer, B. D., D. C. Nobes, and B. G. Warner. 1994. A study of the geoelectrical properties of
787 peatlands and their influence on ground-penetrating radar surveying. *Geophysical*
788 *Prospecting* **42**:179-209.
789 van der Werf, G. R., D. C. Morton, R. S. DeFries, L. Giglio, J. T. Randerson, G. J. Collatz, and
790 P. S. Kasibhatla. 2009. Estimates of fire emissions from an active deforestation region in
791 the southern Amazon based on satellite data and biogeochemical modelling.
792 Wahyunto, S. Ritung, and H. Subagio. 2003. Peta Luas Sebaran Lahan Gambut dan Kandungan
793 Karbon di Pulau Sumatera/Maps of Area of Peatland Distribution and Carbon Content in
794 Sumatera, 1990-2002. Wetlands International e Indonesia Programme and Wildlife
795 Habitat Canada (WHC), Bogor.
796 Wahyunto, S. Ritung, and H. Subagio. 2004. Peta Sebaran Lahan Gambut, Luas dan Kandungan
797 Karbon di Kalimantan/Map of Peatland Distribution Area and Carbon Content in
798 Kalimantan, 2000-2002. Wetlands International - Indonesia Programme and Wildlife
799 Habitat Canada (WHC), Bogor.
800 Warner, B. G., D. C. Nobes, and B. D. Theimer. 1990. An application of ground penetrating
801 radar to peat stratigraphy of Ellice Swamp, southwestern Ontario. *Canadian Journal of*
802 *Earth Science* **27**:932-938.
803 Yu, Z., J. Loisel, D. P. Brosseau, D. W. Beilman, and S. J. Hunt. 2010. Global peatland
804 dynamics since the Last Glacial Maximum. *Geophys. Res. Lett* **37**:doi:10.1029/
805 2010GL043584.

806

807 **Table 1:** Summary of field sites including landcover, peat depth (from direct core measurements) and
808 land system after RePPPProT, Regional Physical Planning Programme for Transmigration..1990.

Study Site	Landcover	Peat depth (m)	Land system	Description
Tanjung Gunung 1 (TG1)	Thinned forest	3.9-4.3	KHY-MDW transition (MDW)	Shallow peat swamps
Tanjung Gunung 2 (TG2)	Rubber plantation	0.3-3.5	KHY-MDW transition (KHY-MDW)	Shallow peat swamps-estuarine/riverine plains

Pelang Forest 1 (P1)	Disturbed forest	4.0-5.0	GBT-MDW boundary	Deep peat swamp- shallow peat swamp
Pelang Forest 2 (P2)	Thinned forest	>9.0	GBT	Deep peat swamp

809

810

811

812 **Table 2:** Summary of cores including coordinates, landcover, peat depth (from direct coring),C stock
813 along the peat profile (in Mg ha⁻¹) and mean % C in the peat layer.

Core	Coordinates (deg)	Landcover	Peat depth (m)	Peat profile C stock (Mg ha ⁻¹)	Mean peat <u>bulk density</u> (g cm ⁻³)	Mean peat C (% C)
TG1.1	Lat: 110.0699 Long: -1.3036	Thinned Forest	4.1	2300.53	<u>0.10</u>	57.74
TG1.2	Lat: 110.0702 Long: -1.3035	Thinned Forest	4.1	2321.39	<u>0.10</u>	59.33
TG2.1	Lat: 110.0631 Long: -1.2986	Rubber plantation	3.0	1662.02	<u>0.11</u>	52.13
TG2.2	Lat: 110.0633 Long: -1.2989	Rubber plantation	3.0	1764.31	<u>0.16</u>	41.60
TG2.3	Lat: 110.0637 Long: -1.2981	Rubber plantation	3.4	1623.72	<u>0.09</u>	54.20
P1.1	Lat: 110.1524 Long: -1.8644	Disturbed Forest	5.0	3039.36	<u>0.13</u>	49.10
P1.2	Lat: 110.1521 Long: -1.8641	Disturbed Forest	4.3	2314.92	<u>0.12</u>	52.46
P2.1	Lat: 110.1272 Long: -1.8999	Thinned Forest	>9.0	5676.67	<u>0.11</u>	57.82
P2.2	Lat: 110.1277 Long: -1.8997	Thinned Forest	8.3	6107.92	<u>0.13</u>	56.12

814

815

816

817 **Figure captions:**

818 **Figure 1:** Schematic showing the location of the Study Sites West Kalimantan, Indonesia. A
819 total of four sites were investigated: Tanjung Gunung Site 1 (TG1) and Site 2 (TG2), and Pelang
820 Forest Site 1 (P1) and Site 2 (P2). Inset shows details about the land system as classified after
821 RePPPProT (1990): Kahayan (KHY) mainly characterized by alluvial plains; and Gambut (GBT),

Formatted: Centered, None, Space Before: 0 pt, Line spacing: single, Don't keep with next, Don't keep lines together

Formatted: Centered, None, Space Before: 0 pt, Line spacing: single, Don't keep with next, Don't keep lines together

Formatted: Centered, None, Space Before: 0 pt, Line spacing: single, Don't keep with next, Don't keep lines together

Formatted: Centered, Space After: 0 pt, Line spacing: single

Formatted: Centered, Space After: 0 pt, Line spacing: single

Formatted: Centered, Space After: 0 pt, Line spacing: single

Formatted: Centered, Space After: 0 pt, Line spacing: single

Formatted: Centered, Space After: 0 pt, Line spacing: single

Formatted: Centered, Space After: 0 pt, Line spacing: single

Formatted: Centered, Space After: 0 pt, Line spacing: single

Formatted: Centered, Space After: 0 pt, Line spacing: single

Formatted: Centered

822 Mendawai (MDW), and Klaru (KLR) characterized by swamps. Color scale indicates elevation
823 above sea level.

824

825 **Figure 2:** GPR common-offset profile using a Mala GPR system with 100 MHz antennae along
826 Line 1 (a) and Line 2 (b). Location of core samples TG1.1 and TG1.2 and inferred units, water
827 table position and presence of wood layers are also shown. Frame highlights the location of a
828 woody area identified along the cores and characterized by the presence of hyperbolic
829 diffractions in the GPR record.

830

831 **Figure 3:** Inverted images of (a) Line 1 and (b) Line 2 resistivity surveys using a four electrode
832 Wenner type array with 1 m electrode spacing. Location of core samples TG1.1 and TG1.2 and
833 inferred units as per Figure 2 are also shown.

834

835 **Figure 4:** (a) GPR common-offset profile using a Mala GPR system with 200 MHz antennae at
836 study Site TG2. Location of two core samples and inferred units are also shown; (b) Inverted
837 image of resistivity survey along the GPR profile in (a) using a four electrode Wenner type array
838 with 1 m electrode spacing.

839

840 **Figure 5:** (a) GPR common-offset profile using a Mala GPR system with 100 MHz antennae at
841 study Site TG2. The profile represents the continuation of the GPR profile shown in Figure 4 (a).
842 | Location of core samples TG2.1-TG2.3 and two additional core samples and inferred units are
843 | also shown. White arrows indicated presence of diffraction hyperbolas; (b) Inverted image of
844 resistivity survey along the GPR profile in (a) using a four electrode Wenner type array with 1 m
845 electrode spacing. Interpreted peat-mineral soil interface is also shown.

846

847 **Figure 6:** GPR common-offset profile using a Mala GPR system with 100 MHz antennae at
848 study Site P1. Location of core sample P1.1 and inferred units and water table position are also
849 shown. Larger white arrow indicates the center of a depressional feature within the reflection
850 record centered between 10-35 m along the profile and 3-5 m depth. Smaller white arrow
851 indicates the presence of a diffraction hyperbola.

852

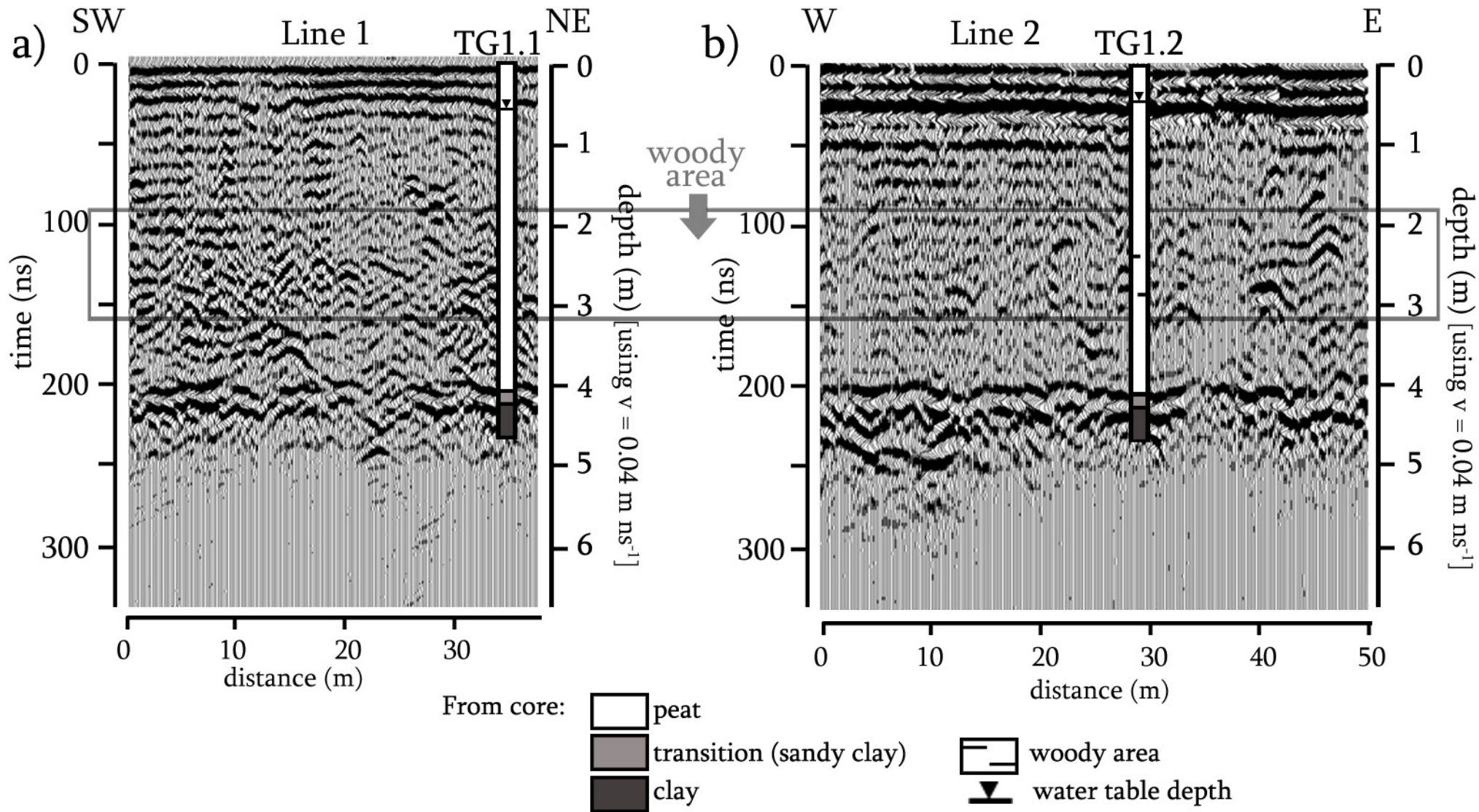
853 **Figure 7:** Inverted image of resistivity survey at Site P1 using a four electrode Wenner type
854 array with 2 m electrode spacing. Note that resistivity profile does not coincide with location of
855 GPR profile shown in Figure 6. Location of core sample P1.2 and inferred units (depicted in
856 | Figure 6) are also shown.

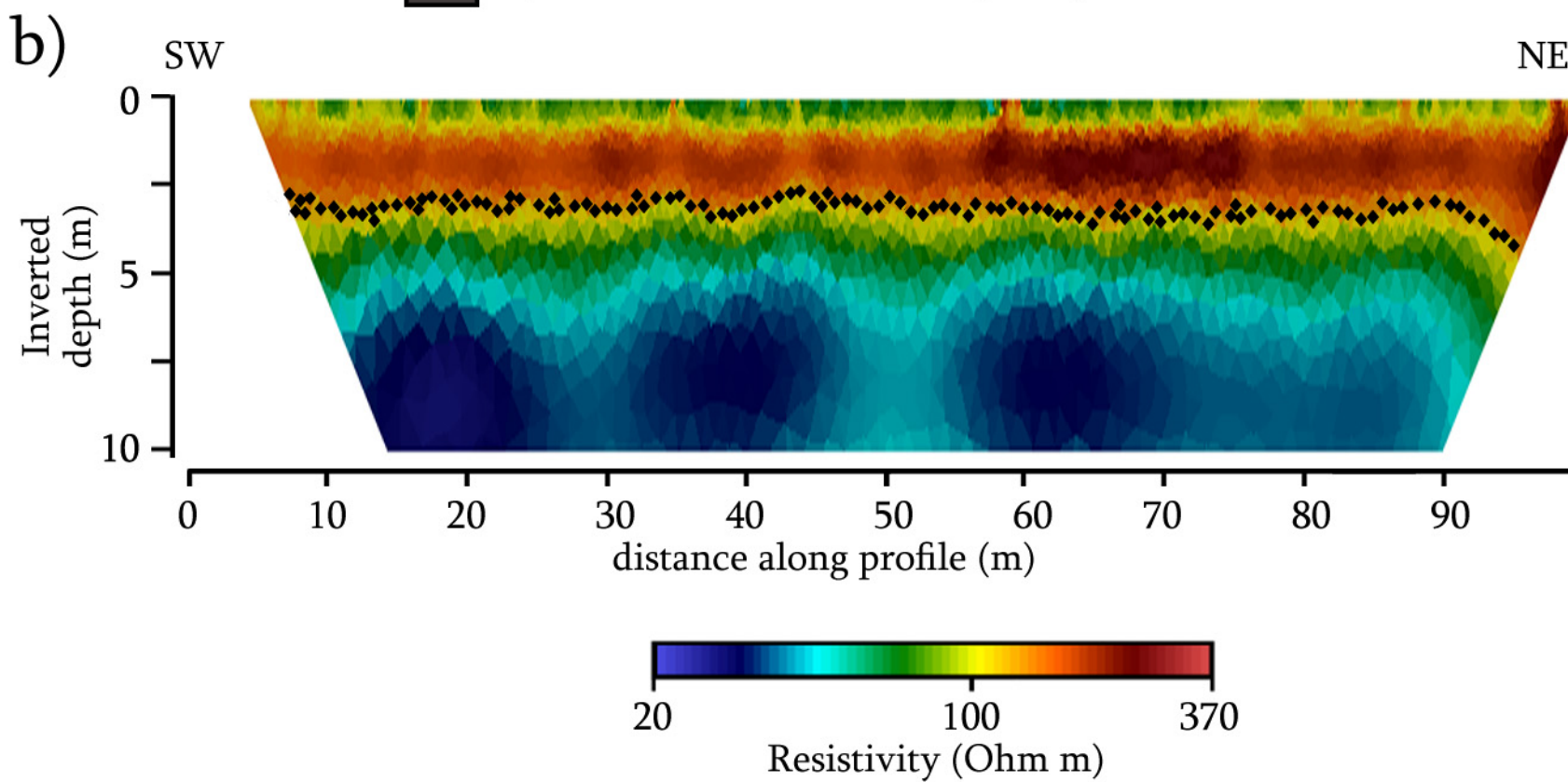
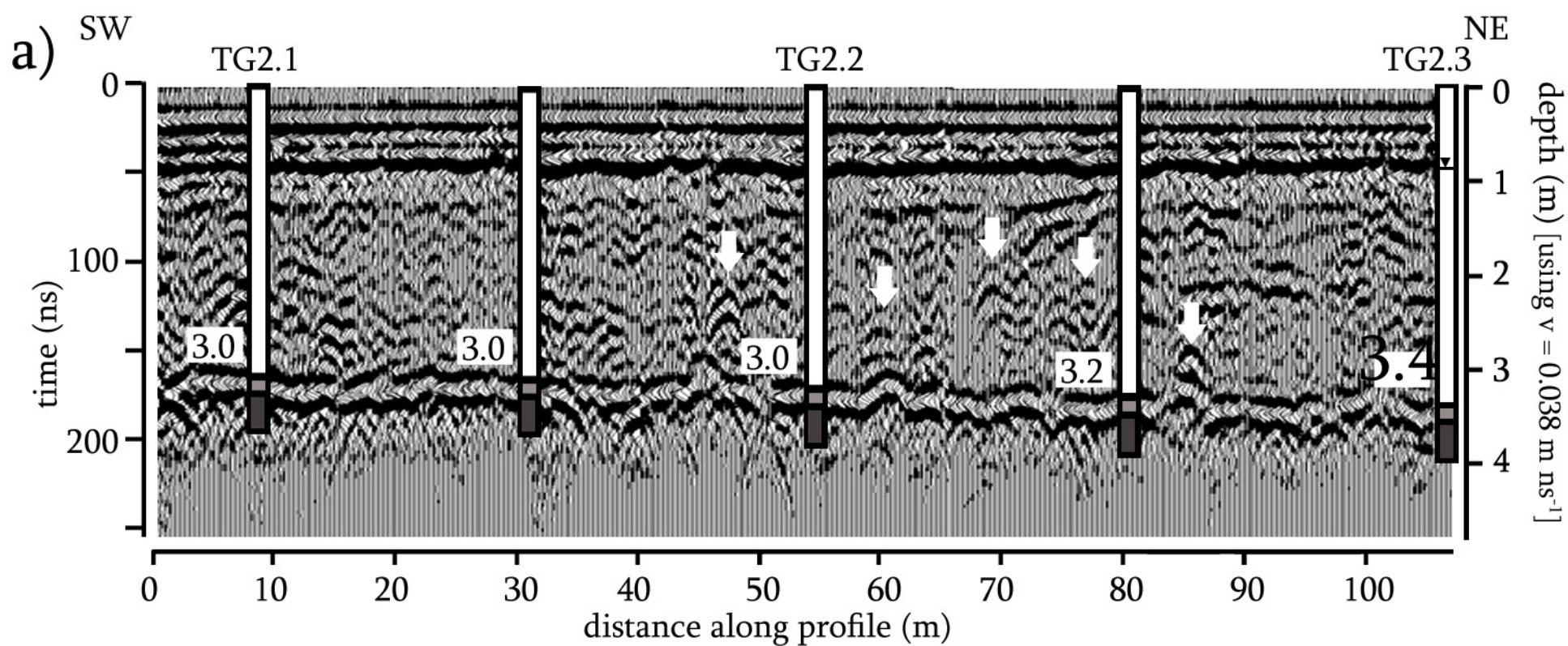
857

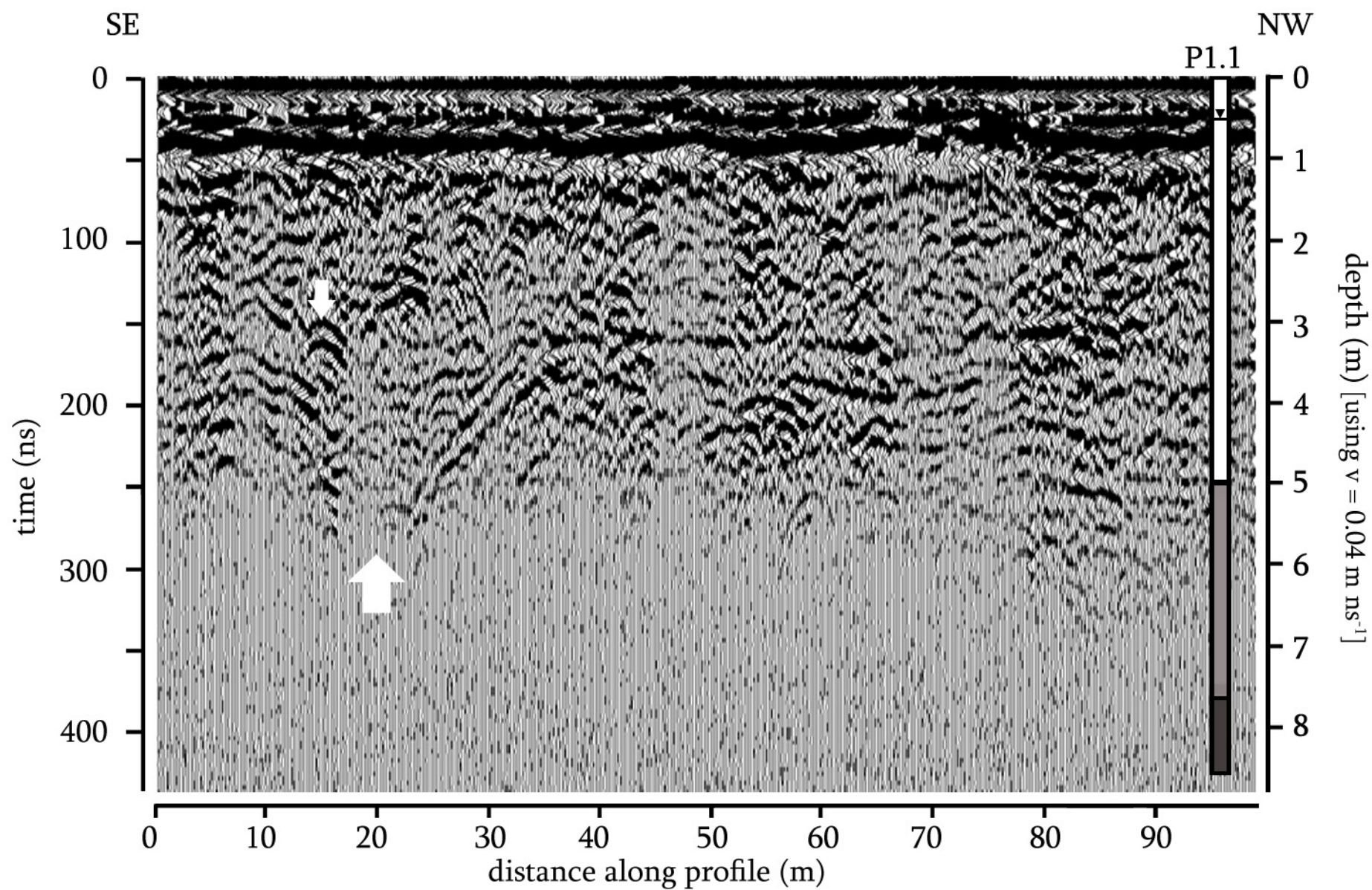
858 **Figure 8:** Inverted image of resistivity survey at Site P2 using a four electrode Wenner type
859 array with 2 m electrode spacing. Location of core sample P2.1, P2.2 and one additional location
860 and inferred units (depicted in Figure 6) are also shown.

861





862 **Figure 9:** Comparison of peat thickness estimated from the a) GPR profile and b) the ERI image
863 as shown in Figure 5 (based on an average velocity of 0.038 m ns^{-1}) and direct coring at 5
864 locations. Error bars in the data were calculated from the difference in peat thickness between
865 GPR using that average velocity and ERI and that measured from the coring. Grey shading
866 indicates estimated surface area from coring.







From core:

	peat		water table depth
	transition (sandy clay)		
	clay		

